Adaptive Behavior
http://adb.sagepub.com/

Moth-inspired plume tracing via multiple autonomous vehicles under formation control

Xiaodong Kang and Wei Li

Adaptive Behavior 2012 20: 131 originally published online 14 February 2012
DOI: 10.1177/1059712311433131

The online version of this article can be found at:
http://adb.sagepub.com/content/20/2/131

Published by:
SAGE
http://www.sagepublications.com

On behalf of:
ISAB
International Society of Adaptive Behavior

Additional services and information for *Adaptive Behavior* can be found at:

Email Alerts: http://adb.sagepub.com/cgi/alerts

Subscriptions: http://adb.sagepub.com/subscriptions

Reprints: http://www.sagepub.com/journalsReprints.nav

Permissions: http://www.sagepub.com/journalsPermissions.nav

Citations: http://adb.sagepub.com/content/20/2/131.refs.html

>> Version of Record - Mar 9, 2012

OnlineFirst Version of Record - Feb 14, 2012

What is This?

Downloaded from adb.sagepub.com at SEIR on August 2, 2012

Original Paper

Adaptive Behavior

Adaptive Behavior
20(2) 131–142
© The Author(s) 2012
Reprints and permissions:
sagepub.co.uk/journalsPermissions.nav
DOI: 10.1177/1059712311433131
adb.sagepub.com
SAGE

Moth-inspired plume tracing via multiple autonomous vehicles under formation control

Xiaodong Kang[1,2] and Wei Li[1,3]

Abstract

The moth-inspired plume-tracing strategies on a single REMUS underwater vehicle successfully tracked a Rhodamine dye plume over 100 m and declared its source location in near-shore ocean environments that are characterized by turbulence, tides, and waves. This paper expands moth-inspired plume tracing via a single vehicle to multiple vehicles. The new strategy includes a mechanism determining a leader vehicle to perform moth-inspired plume-tracing maneuvers and a formation algorithm controlling non-leaders to follow the leader during plume-tracing missions. The Monte Carlo studies evaluate the strategy in a virtual environment where a simulated plume with significant filament intermittency and meander is developed. Considering our application, our simulation studies address an autonomous underwater vehicle's kinematics and dynamics. The results demonstrate plume-tracing performance achieved by multiple vehicles, which automatically switch their roles superior to the single vehicle.

Keywords

Insect-inspired robot, robotics plume tracing, formation control, multiple autonomous vehicles, odor plume

1 Introduction

Olfactory-based mechanisms have been hypothesized for biological behaviors, e.g., foraging by lobsters (Basil & Atema, 1994), foraging by blue crabs (Weissburg & Zimmer-Faust, 1994), mate seeking, and foraging by moths (Cardé, 1996). A review on insect finding distant, wind-borne sources of odor can be found in the recent article by Cardé and Willis (2008). Koehl et al. (2001) further reported how lobster olfactory antennules hydro-dynamically alter the spatiotemporal patterns of concentration in turbulent odor plumes.

Recently there has been interest in developing autonomous vehicles capable of chemical plume tracing (CPT) (Cowen & Ward, 2002). Vergassola, Villermaux, and Shraiman (2007) generalized the plume-tracing issue as "infotaxis" as a strategy for searching without gradients. The work by Belanger and Willis (1998) presented plume-tracing strategies, including counter-turning strategies, intended to mimic moth behavior, and analyzed the performance in a computer simulation. Li, Farrell, and Cardé (2001) evaluated and optimized the moth-inspired plume-tracing strategies in a simulated plume with significant meander and intermittency of plume puffs. Grasso, Consi, Mountain, and Atema (2000) evaluated biomimetic strategies and challenged theoretical assumptions of the strategies by implementing biomimetic strategies on their robot lobster. The studies by Liao and Cowen (2002) and Weissburg et al. (2002) proposed sensor array-based strategies and suggested that search strategies based on following the "edge" of a plume (as opposed to the centerline) are robust. Russell (2001) included robotic implementation of algorithms that estimate statistics of the plume such as the plume centroid, and experiments where the chemical is constrained to a multiple-duct tunnel system. Ishida, Kagawa, Nakamoto, and Moriizumi (1996) used an array of sensors to track the plume by estimating the three-dimensional direction toward the odor source. Marques, Nunes, and Almeida (2002) performed plume-tracing tests using mobile robots in laboratory environments. Lilienthal, Ulmer, Froehlich, Werner, and Zell (2004) reported test results

[1]State Key Laboratory of Robotics, Shenyang Institute of Automation, Chinese Academy of Sciences, Liaoning Province, China
[2]Graduate School of the Chinese Academy of Sciences, Beijing, China
[3]Department of Computer Engineering and Science, California State University, Bakersfield, CA, USA

Corresponding author:
Wei Li, Department of Computer and Electrical Engineering and Computer Science, California State University, Bakersfield, CA 93311, USA
Email: wli@csub.edu

Downloaded from adb.sagepub.com at SEIR on August 2, 2012

on proximity to a gas source when a laboratory robot maneuvered in the vicinity of the source location. Two research groups addressed CPT via multiple robots through swarm behaviors (Hayes, Martinoli, & Goodman, 2002; Zarzhitsky & Spears, 2005). Recently, Meng, Yang, Wang, and Zeng (2011) used multi-robots to localize an odor source in airflow environments.

Autonomous underwater vehicles (AUVs) with CPT capabilities would be valuable in searching for deep-sea hydrothermal vents, finding unexploded ordnance in near-shore environments, and monitoring pollutants or localizing sources of hazardous chemicals in a harbor. The strategies proposed in the article (Li et al., 2001) were implemented on a REMUS underwater vehicle with a single chemical sensor for the in-water test runs in November and April 2002 at the San Clemente Island of California and in June 2003 in Duck, North Carolina (Li, Farrell, Pang, & Arrieta, 2006; Farrell, Pang, & Li, 2005). The field experiments successfully demonstrated tracking of chemical plumes over 100 m and source identification accuracy in the order of tens of meters in the near-shore, oceanic fluid flow environments, where plumes were developed under turbulence, tides and waves. The most recent CPT in-water test run via an AUV at Dalian Bay in China (Kang, Li, Xu, Feng, & Li, 2011) also validated effectiveness of the moth-inspired CPT strategies.

The effective tracking of a chemical plume via multiple AUVs in ocean environments is a very challenging task. Based on the moth-inspired approaches that successfully tracked a chemical plume and declared the chemical source in the near-shore ocean environments, however, developing a new strategy for plume tracing via multiple AUVs allows us to simplify the design procedure. Effectively coordinating multiple AUVs to achieve a better CPT performance has become one of the most important issues. This paper extends moth-inspired plume tracing via a single vehicle to multiple vehicles by redefining the Find-Plume, Maintain-Plume, Reacquire-Plume, and Declare-Source behaviors (Li et al., 2006). Under the assumption of communication availability between the vehicles, we develop a coordination mechanism for selecting a leader among multiple vehicles, which leads the vehicle fleet to perform moth-inspired plume tracing and propose a formation algorithm for the control of the non-leader vehicles to follow the leader during CPT missions. We evaluate the proposed strategy in a simulated fluid-advected environment with scales of 100 m. The studies show that, in comparison with a single vehicle, CPT via a multiple-vehicles system significantly reduces the time cost for tracing the plume toward its source and identifying the source location, and slightly improves the accuracy of the declared source locations. Figure 1 shows a scenario of tracing a plume with a significant meander via multiple vehicles.

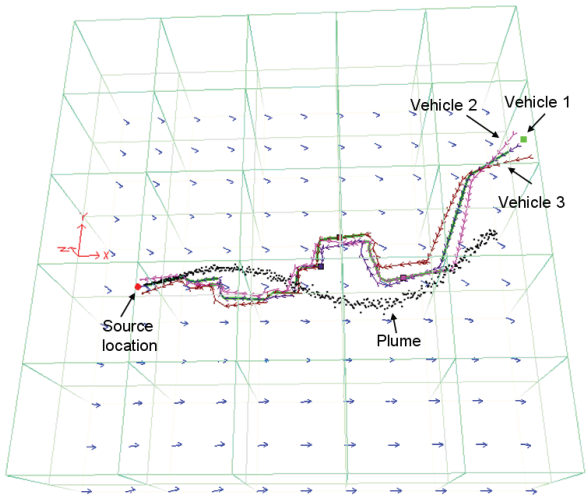

Figure 1. Tracking of a chemical plume with a significant meander via multiple vehicles. The vehicles automatically switch their roles to effectively trace the plume. A leader is controlled to stay in the middle between two followers during the chemical plume-tracing mission.

This paper is organized as follows. Section 2 briefly reviews the moth-inspired CPT strategy. Section 3 presents the kinematics model for formation control of multiple vehicles. Section 4 develops a coordinate mechanism for multiple vehicles and a control law in regards to an AUV's kinematics for keeping multiple vehicles in a formation shape. Section 5 uses the Monte Carlo method to evaluate the proposed strategy by considering the AUV's dynamics. Section 6 draws some conclusions about the strategy and the test runs' results.

2 Moth-inspired plume tracing

The moth-inspired CPT strategies (Li et al., 2001, 2006) consist of four fundamental behaviors: finding the plume (Find-Plume), maintaining the plume (Maintain-Plume), reacquiring the plume (Reacquire-Plume), and declaring the source location (Declare-Source). The Find-Plume behavior is designed to dominantly implement a cross-flow search for the entire operational area without any assumptions about the location of the plume source. The commanded heading is defined as $\theta = w_d(t,x,y) + sign(\eta)\Delta\theta(t)$, which is an offset to the computed flow direction denoted by $w_d(t,x,y)$. The sign of the variable η will be ± 1. The variable $\Delta\theta(t)$ can only take on one of the two constant values $\Delta\theta(t)_{\text{up}}$ or $\Delta\theta(t)_{\text{down}}$. How to choose an initial direction to start the Find-Plume behavior is discussed in Li et al. (2006). The Maintain-Plume and Reacquire-Plume behaviors are abstracted from the location of the pheromone-emitting females by flying male moths (Cardé, 1996; Elkinton, Schal, Onto, & Cardé, 1987). The Maintain-Plume behavior is described by

Downloaded from adb.sagepub.com at SEIR on August 2, 2012

$$\begin{cases} \theta = w_d(t,x,y) + 180^\circ + \Delta\theta(t)_{\text{Track-In}} & t \in T_{\text{above}} \\ v = v_c \end{cases} \quad (1)$$

$$\begin{cases} \theta = w_d(t,x,y) + 180^\circ + \Delta\theta(t)_{\text{Track-Out}} & t \in T_{\text{below}} \\ v = v_c \end{cases} \quad (2)$$

where $w_d(t,x,y)$ is the flow direction, both $\Delta\theta(t)_{\text{Track-In}}$ and $\Delta\theta(t)_{\text{Track-Out}}$ are the offset angles for Track-In and Track-Out activities, and T_{above} and T_{below} are durations for Track-In and Track-Out activities. The Reacquire-Plume behavior reacquires a contact with the plume in the situation where the chemical has not been detected for at least a few seconds. A cloverleaf-shaped trajectory or its variant (Li et al., 2001, 2006) was used to implement the Reacquire-Plume behavior to cast for the lost chemical plume. The Declare-Source algorithms are derived from the moth-inspired plume-tracing strategies (Li, 2010). These algorithms use the last chemical detection points (LCDPs) to construct source identification zones for source identification. A chemical detection point at which a vehicle loses contact with the chemical plume for certain seconds is defined as LCDP. In this paper, we implement the SIZ_F source identification algorithm based on LCDPs for CPT missions. The SIZ_F algorithm maintains all LCDPs in the order of the current up-flow direction using the priority queue. The SIZ_F algorithm declares the source location when enough LCDPs, i.e., the number of LCDPs $\geq N_{\min}$, are located in a source identification zone with a radius ε_F. We take $N_{\min} = 6$ and $\varepsilon_F = 6$ m as suggested in the article by Li (2010). This algorithm was validated through our recent in-water test runs of tracing a Rhodamine dye plume via a single AUV (Kang et al., 2011).

3 Formation control of multiple vehicles

In contrast to CPT via multiple vehicles (Hayes et al., 2002; Zarzhitsky & Spears, 2005), we adopt the leader–follower strategy (Edwards, Bean, Odell, & Anderson, 2004) to perform CPT missions via multiple vehicles. This strategy suits the control of swarm behaviors of the entire vehicle fleet and can guarantee the formation stability, as the leader can be replaced with a follower when it is defective. A formation approach maintains control of the multiple vehicles in two levels. Firstly, it determines a sub-target for the leader according to the current vehicles' status, and then generates trajectories to steer the vehicles toward the target in a formation shape depending on a control strategy.

Considering our further application of CPT via multiple AUVs in near-shore ocean environments, we establish the kinematic equations of the AUV to describe relative motions of the leader and a follower. In doing so, we define two types of coordinate systems: the world system $\{0\}$ and a body system $\{i\}$ defined on a follower vehicle i, as depicted in Figure 2. Let (v, ψ, θ) be the vehicle's status, described in $\{0\}$, where v is the forward velocity in m/s, ψ is yaw angle in radians, and θ is pitch angle in radians respectively, assuming the vehicle's roll angle $\varphi = 0$.

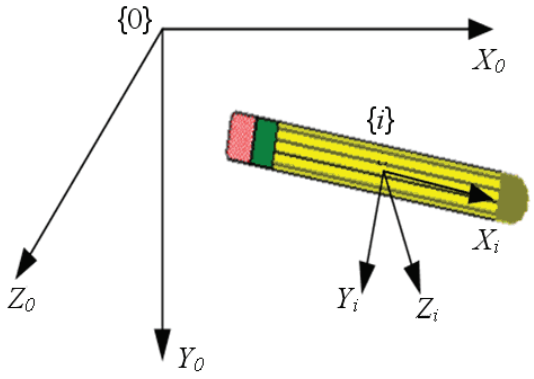

Figure 2. World coordinate systems $\{0\}$ and a body coordinate system $\{i\}$ on vehicle i.

The general rotation matrix from the world coordinate system $\{0\}$ to the body coordinate system $\{i\}$ can be expressed by

$$ {}^{i}_{0}R = \begin{bmatrix} \cos\theta_i \cos\psi_i & \cos\theta_i \sin\psi_i & -\sin\theta_i \\ -\sin\psi_i & \cos\psi_i & 0 \\ \sin\theta_i \cos\psi_i & \sin\theta_i \sin\psi_i & \cos\theta_i \end{bmatrix} \quad (3)$$

The velocity equations of vehicle i described in 0 can be found by

$$\begin{cases} \dot{x}_i = v_i \cos\theta_i \cos\psi_i \\ \dot{y}_i = v_i \cos\theta_i \sin\psi_i \\ \dot{z}_i = -v_i \sin\theta_i \end{cases} \quad (4)$$

Equation (4) can be written as

$$\dot{p}_i = A(\theta_i, \psi_i) v_i \quad (5)$$

where $A(\theta_i, \psi_i) = [cos\theta_i cos\psi_i \quad cos\theta_i sin\psi_i \quad -sin\theta_i]^T$. The position vector $p_i = [x_i, y_i, z_i]^T$ of vehicle i, described in system $\{0\}$ can be obtained, by integral of Equation 5. We use

$$\Delta p^f = {}^{f}_{0}R(p_l - p_f) \quad (6)$$

to calculate the relative distance vector $\Delta p^f = [\Delta x^f, \Delta y^f, \Delta z^f]^T$ from a follower f to the leader l, described in the follower's body coordinate system $\{f\}$, where ${}^{f}_{0}R$ is the rotation mapping from the world coordinate system $\{0\}$ to the follower body system $\{f\}$. Note that subscript i indicates that the status of vehicle i is described in the world coordinate system $\{0\}$, whereas superscript f is described in the follower body system $\{f\}$. Figure 3a shows projections of the leader relative position on its two followers' body coordinate

Downloaded from adb.sagepub.com at SEIR on August 2, 2012

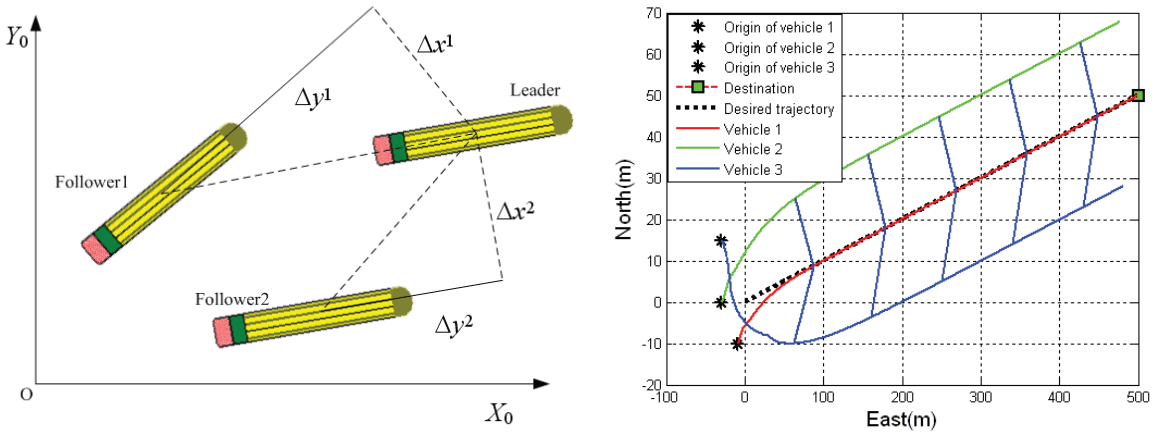

(a) (b)

Figure 3. Formation control of three autonomous underwater vehicles (AUVs) in a triangle shape. (a) The leader location is described in the coordinate systems of the followers. (b) The leader's trajectory is indicated by the red line (middle) and the followers' trajectories by the green and blue lines on two sides of the leader's trajectory.

systems. Figure 3b shows the trajectories of the three autonomous vehicles under the formation control laws described in Equation 16. The leader, located in the middle along the motion direction, is moving on a linear trajectory indicated by the red trajectory, whereas both of the two followers follow the leader on both of its sides and generate the green and blue trajectories.

4 Chemical plume tracing via multiple vehicles

For CPT missions via multiple autonomous vehicles, we re-define the Find-Plume, Maintain-Plume, Reacquire-Plume, and Declare-Source behaviors below. The Find-Plume behavior controls the multiple vehicles to search for a plume in the entire operational area using cross-flow trajectories without any assumptions about the location of the chemical plume and its source. The Reacquire-Plume behavior controls the multiple vehicles to follow a cloverleaf-shaped trajectory or its variation to cast the lost plume. Obviously, the Find-Plume or the Reacquire-Plume maneuvers using multiple AUVs increase the chance of finding or casting the plume. The multiple vehicles system activates its Maintain-Plume behavior once one of the vehicles detects a chemical plume. During Maintain-Plume maneuvers, the leader vehicle utilizes the Track-In and Track-Out activities to move up-flow toward the source location, whereas the non-leader vehicles server as guarders to follow the leader. For chemical source declaration via the multiple AUVs, the inputs to the SIZ_F algorithm are the LCDPs collected by all the AUVs, instead of a single one. Only the leader AUV declares the source location. Its pseudo code is given in Table 1. The AUVs' roles are assigned at activating the Maintain-Plume behavior. The source identification behavior does not change their roles. For the Find-Plume behavior, we use

$$\begin{aligned} A_i &= rand() \\ A_{\max} &= max(A_i), i = 1, \cdots, n \end{aligned} \tag{7}$$

to choose the leader, where A_i is the leader competition coefficient of vehicle i, $rand()$ generates a random number between 0 and 1, $A_{\max}$ is the maximum among all competition coefficients, and the vehicle with $A_{\max}$ is the leader. For the Maintain-Plume behavior, we use

$$\begin{aligned} A_i &= \begin{cases} 0, & C_i < \delta \\ \alpha u(C_i - \delta) - \beta(e^{-kD_i} - 1), & C_i \geq \delta \end{cases} \\ A_{\max} &= max(A_i), i = 1, \cdots, n \end{aligned} \tag{8}$$

to choose the leader, where δ is the threshold defined for chemical sensor, D_i is chemical detected time for vehicle i, α, β, and k are the positive constants, $u(C_i - \delta)$ is a unit-step function and its output is 1 when $C_i \geq \delta$, and C_i is the chemical concentration detected by vehicle i and its model is discussed in the work by Li et al. (2001). Compared with the time lag of the vehicle dynamics, the chemical sensor's response time can be ignored. In our study, we choose $\alpha = \beta = 0.5$ and $k = 1.0$. Equation 8 selects the vehicle that first detects the chemical plume as the leader to start the Maintain-Plume behavior during the course of a CPT mission. When a vehicle is selected as the leader, it should be controlled to stay in the middle between the two followers during CPT missions, whereas the two followers follow and keep a distance from the leader, as shown in

Downloaded from adb.sagepub.com at SEIR on August 2, 2012

Table 1. SIZ_F algorithm for identifying the plume source via an AUV fleet

ALGORITHM SIZ_F(Q_1**[1,… $N_{all(1)}$], …, Q_n[1,… $N_{all(n)}$])**

//Identifying the source location by **SIZ_F** *algorithm via an* AUV fleet.

//n is the vehicle number in the AUV fleet, including the leader and followers.

//Input: Priority queue **Q[1,… N_{all}]**, *where* $N_{all} = \sum_{i=1}^{n} N_{all(n)}$.

//Output: Status of source identification.

if ($N_{all} \geq N_{ini}$)

Sort Q in the order of the current up-flow direction

L[1,… N_{all}] ← **Q[1,… N_{all}]** ; n_1 ← N_{all} *// L is a list*

status ← **false**

while $n_1 \geq N_{min}$ **do**

Calculate the mean value $(x_{last}^{(m)}, y_{last}^{(m)})$ *of all* **LCDP***s in the queue;*

Find the **LCDP** $p_{\max}$ *with the largest distance* $D_{\max}$ *to* $(x_{last}^{(m)}, y_{last}^{(m)})$;

if $D_{\max} > \varepsilon_F$

remove $p_{\max}$ *from L;* $n_1 \leftarrow n_1 - 1$

else

status ← **true; break**

if *status* = **true**

return $(x_{last}^{f(1)}, y_{last}^{f(1)})$ *as the source location*

else

return *no source location identified*

else

return *no source location identified*

Figure 3b. The Reacquire-Plume behavior keeps the same leader determined by Equation 8.

The proposed strategy for the plume tracing via multiple vehicles inherits the demonstrated advantage of the moth-inspired plume tracing via a single vehicle, i.e., it uses a leader in the multiple vehicles system to perform the Find-Plume, Maintain-Plume, Reacquire-Plume, and Declare-Source behaviors. Being superior to the single vehicle system, the multiple vehicles system determines dynamically its leader during the course of CPT missions according to the vehicles' statuses and environment information so that each vehicle in the multiple vehicles system potentially acts as a leader. Through communication between the vehicles, the leader has to direct the non-leaders to find the plume, trace the plume, cast the plume, and declare the plume source location. Figure 4 shows the behavior switching diagram-based coordination mechanism for a multi-vehicle system, which is designed by adding a Formation-Keeping behavior to the diagram for a single vehicle system (Farrell et al., 2005). The symbol d denotes the behavior switch that is on when chemical is detected, s denotes the behavior switch that turns on when source is declared, c denotes the behavior switch that is on when the vehicle's role is switched, $\bar{d}$ denotes the behavior switch that is on when chemical is not detected for some time interval, $\bar{s}$ denotes the behavior switch that is on when source is not declared, and the symbol $\bar{c}$ denotes the behavior switch that is on when the vehicle's role remains unchanged. Once the leader changes its role, it acts as a follower by switching its behavior to Formation-Keeping. For the followers, their fundamental behavior is Formation-Keeping. Each follower probably switches its role into that of a leader when it triggers a Track-In activity, as

Downloaded from adb.sagepub.com at SEIR on August 2, 2012

indicated by a dash-dot arrow labeled with $d \cap c$ in Figure 4, and at the same time the former leader becomes a follower.

In our application, we use three autonomous vehicles to perform CPT missions while maintaining a triangular formation. In order to implement the Formation-Keeping behavior, we calculate the deviations of the relative distance vector in Equation 6 and then obtain the velocity vector

$$\begin{aligned}\Delta\dot{p}^f &= {}^f_0R(\dot{p}_l - \dot{p}_f) + {}^f_0\dot{R}(p_l - p_f)\\ &= {}^f_0R \cdot \dot{p}_l - {}^f_0R \cdot \dot{p}_f + {}^f_0\dot{R}(p_l - p_f)\end{aligned} \tag{9}$$

where $p_l = [x_l, y_l, z_l]^T$ and $p_f = [x_f, y_f, z_f]^T$ are the locations of the leader and the follower described in the world coordinate system, and $\Delta\dot{p}^f$ is described in the follower coordinate system $\{f\}$, respectively. Considering the orthogonality of ${}^f_0R$ and using Equations 5 and 6, we have

$$\Delta\dot{p}^f = {}^f_0R \cdot A(\theta_l, \psi_l)v_l - {}^f_0R \cdot A(\theta_f, \psi_f)v_f + {}^f_0\dot{R}({}^f_0R)^T\Delta p^f \tag{10}$$

and

$${}^f_0R \cdot A(\theta_l, \psi_l) = \begin{bmatrix} \cos\theta_f\cos\psi_f & \cos\theta_f\sin\psi_f & -\sin\theta_f \\ -\sin\psi_f & \cos\psi_f & 0 \\ \sin\theta_f\cos\psi_f & \sin\theta_f\sin\psi_f & \cos\theta_f \end{bmatrix} \cdot \begin{bmatrix} \cos\theta_l\cos\psi_l \\ \cos\theta_l\sin\psi_l \\ -\sin\theta_l \end{bmatrix} = \begin{bmatrix} \cos\theta_l\cos\theta_f\cos\Delta\psi + \sin\theta_l\sin\theta_f \\ \cos\theta_l\sin\Delta\psi \\ \cos\theta_l\sin\theta_f\sin\Delta\psi - \sin\theta_l\cos\theta_f \end{bmatrix} \tag{11}$$

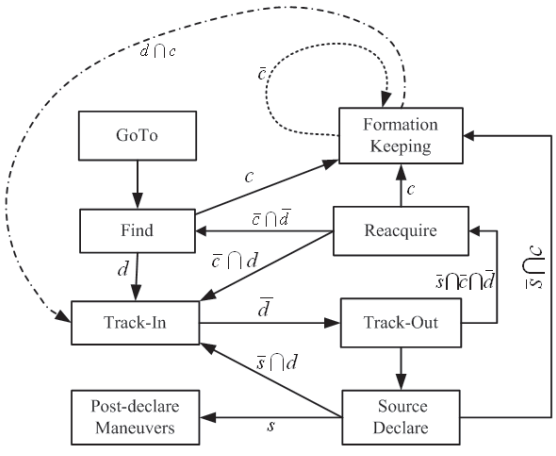

Figure 4. Behavior switching diagram-based coordination mechanism for multiple vehicles to trace a chemical plume.

$${}^f_0R \cdot A(\theta_f, \psi_f) = \begin{bmatrix} \cos\theta_f\cos\psi_f & \cos\theta_f\sin\psi_f & -\sin\theta_f \\ -\sin\psi_f & \cos\psi_f & 0 \\ \sin\theta_f\cos\psi_f & \sin\theta_f\sin\psi_f & \cos\theta_f \end{bmatrix} \cdot \begin{bmatrix} \cos\theta_f\cos\psi_f \\ \cos\theta_f\sin\psi_f \\ -\sin\theta_f \end{bmatrix} = \begin{bmatrix} 1 \\ 0 \\ 0 \end{bmatrix} \tag{12}$$

$${}^f_0\dot{R} \cdot ({}^f_0R)^T = \begin{bmatrix} r_{11} & r_{12} & r_{13} \\ r_{21} & r_{22} & r_{23} \\ r_{31} & r_{32} & r_{33} \end{bmatrix} \begin{bmatrix} \cos\theta_f\cos\psi_f & -\sin\psi_f & \sin\theta_f\cos\psi_f \\ \cos\theta_f\sin\psi_f & \cos\psi_f & \sin\theta_f\sin\psi_f \\ -\sin\theta_f & 0 & \cos\theta_f \end{bmatrix} = \begin{bmatrix} 0 & \dot{\psi}_f\cos\theta_f & -\dot{\theta}_f \\ -\dot{\psi}_f\cos\theta_f & 0 & -\dot{\psi}_f\sin\theta_f \\ \dot{\theta}_f & \dot{\psi}_f\sin\theta_f & 0 \end{bmatrix} \tag{13}$$

where $\Delta\psi = \psi_f - \psi_l$ and

$$\begin{cases} r_{11} = -\dot{\theta}_f\sin\theta_f\cos\psi_f - \dot{\psi}_f\cos\theta_f\sin\psi_f \\ r_{12} = -\dot{\theta}_f\sin\theta_f\sin\psi_f + \dot{\psi}_f\cos\theta_f\cos\psi_f \\ r_{13} = -\dot{\theta}_f\cos\theta_f \\ r_{21} = -\dot{\psi}_f\cos\psi_f \\ r_{22} = -\dot{\psi}_f\sin\psi_f \\ r_{23} = 0 \\ r_{31} = \dot{\theta}_f\cos\theta_f\cos\psi_f - \dot{\psi}_f\sin\theta_f\sin\psi_f \\ r_{32} = \dot{\theta}_f\cos\theta_f\sin\psi_f + \dot{\psi}_f\sin\theta_f\cos\psi_f \\ r_{33} = -\dot{\theta}_f\sin\theta_f \end{cases} \tag{14}$$

Plugging the Equations 11–13 into 10, we have

$$\Delta\dot{p}^f = \begin{bmatrix} \sin\theta_f\sin\theta_l + \cos\theta_f\cos\theta_l\cos\Delta\psi \\ \cos\theta_l\sin\Delta\psi \\ -\sin\theta_f\sin\theta_l + \cos\theta_f\cos\theta_l\cos\Delta\psi \end{bmatrix} v_l + \begin{bmatrix} -1 & -\Delta x^f & \Delta y^f\cos\theta_f \\ 0 & 0 & -\Delta x^f\cos\theta_f - \Delta z^f\sin\theta_f \\ 0 & \Delta z^f & \Delta y^f\sin\theta_f \end{bmatrix} \begin{bmatrix} v_f \\ \dot{\theta}_f \\ \dot{\psi}_f \end{bmatrix} \tag{15}$$

When the distance of a follower to the leader is assigned, i.e., $\Delta\dot{p}^f$ in Equation 15 is given, we can obtain the formation control law for a follower (Cui, Xu, Xu, Yan, & Pan, 2007):

$$\begin{cases} v_f = (\sin\theta_f\sin\theta_l + \cos\theta_f\cos\theta_l\cos\Delta\psi)v_l + \gamma^2 x_e \\ \dot{\theta}_f = z_e v_l\cos\theta_l\cos\Delta\psi/k_2 + \Delta z^f\sin\theta_f - k_2\sin\theta_f + \dot{\theta}_l \\ \dot{\psi}_f = v_l y_e\cos\theta_l/k_1 + (k_1\sin\Delta\psi - z_e\Delta y^f\sin\theta_f) + \dot{\psi}_l \end{cases} \tag{16}$$

where x_e and y_e represent the formation errors between the follower's actual location and the trajectory to be followed on the axes X and Y, and the control coefficients γ, k_1 and k_2 are positive constants that mainly affect the forward velocity, the yaw angle and pitch angle rates of the follower. In our application, we

Downloaded from adb.sagepub.com at SEIR on August 2, 2012

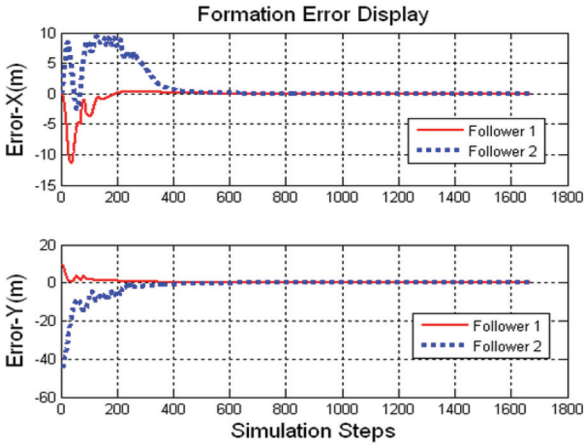

Figure 5. Simulation studies on following trajectories under formation control of the non-leader vehicles.

choose $\gamma = 16$, $k_1 = 0.1$ and $k_2 = 0.01$. By considering the vehicle's dynamics (Kang, 2010), we simulate different formation strategies to evaluate the formation performance. During the simulation studies, the leader's velocity is set as constant 6 knots, whereas the followers' velocities are adjusted to between 1 and 8 knots (0.5–4.0 m/s) to maintain the assigned formation. Figure 5 represents a simulation result on maintaining a triangular formation. It clearly demonstrates that using the proposed control law the formation errors are eliminated quickly. For in-water test runs, we use data collected by the Doppler Velocity Log (DVL) to calculate the actual vehicle's location (Li et al., 2006; Farrell et al., 2005; Kang et al., 2011; Tian, Li, Zhang, & Yu, 2011). This localization technique can be directly applied for each AUV in the multiple AUV system.

5 Simulation evaluation

We evaluate the strategy for moth-inspired CPT via multiple vehicles in a simulated fluid-advected environment (Sutton & Li, 2008), which upgrades the version of Farrell, Murlis, Long, Li, and Cardé (2002) by expanding the filament-based plume model from two dimensions to three dimensions. The upgraded version allows us conveniently to define multiple vehicles and plume sources, as shown in Figure 6. The plume model (Farrell et al., 2002) does not specify any type of plume, but addresses the major characters that challenge CPT algorithms, such as significant intermittency between chemical filaments, significant plume meander, noise and uncertainty of sensors, and magnitude and direction variation of flow fluid at time and location. The detailed analysis of this model and the data comparison between the simulated and real plumes can be found in Farrell et al. (2002).

The operational area is specified by $[0, 100] \times [-50, 50]$ in meters. The filament release rate is 5 filaments per second, the simulation time step is 0.01 s, and the mean fluid velocity is 1.0 m/s. The measured fluid flow is corrupted by additive noise that is a white normal random process. The plume source is located at (10, 0) in meters, which is unknown to the vehicles fleet. The home location is defined as (110, 40) in meters outside the operational area. The operation time is limited to $T_{\max} = 1000$ s. For each CPT mission, the vehicle fleet starts around the home location and returns to the home location when the vehicle fleet identifies the source location or reaches its maximum mission time $T_{\max}$.

The evaluation studies are to compare the CPT performances via a single vehicle with those via multiple vehicles. Both strategies run in the same simulated fluid-advected environment concurrently. The simulation studies keep changing the chemical plume in a fluid environment over time, and 1000 CPT test runs are performed for our studies. Vehicle speed can be adjusted between 1 and 8 knots (between 0.5 and 4.0 m/s). Figure 6 shows a run of the CPT mission, including the Find-Plume, Maintain-Plume, Reacquire-Plume, and Declare-Source behavior activities. The vehicle fleet starts its CPT mission around the home location. Vehicle 1 is selected as the leader and activates Find-Plume behavior, and vehicles 2 and 3 follow the leader to perform a cross-flow search for the chemical plume in the operational area. Since vehicle 3 first detects the plume, it becomes the leader, as shown in Figure 6a. Once vehicle 3 activates Maintain-Plume behavior as the new leader and uses Track-In and Track-Out activities toward the chemical source location, while the other vehicles start to follow the new leader via communication. For example, vehicle 1 switches its role to a follower, so it moves to the left side of the leader to build another triangular formation and maintains this formation by following the leader, as shown in Figure 6b. When vehicle 3 loses its contact with the chemical for a certain number of seconds, it activates Reacquire-Plume behavior to cast for the lost chemical, and vehicles 1 and 2 follow the leader on cloverleaf-shaped trajectories. As vehicle 2 first casts the lost plume during Reacquire-Plume activity, it switches its role to the leader and triggers a new Maintain-Plume activity. In the meantime, vehicle 3 turns its role to that of a follower and moves to the right side to build a new triangular formation. Vehicle 2 leads the vehicle fleet to reach the source location, as shown in Figure 6c. Figure 6d demonstrates Declare-Source activities of the vehicle fleet to identify the source location. Figure 1 shows the more difficult tracking of the chemical plume related to a significant meander via multiple vehicles. Tables 2 and 3 list the result of the evaluation studies in three aspects: reliability, accuracy, and time cost. The results show that CPT via the multiple vehicles significantly reduces the time cost for tracing the plume and declaring the source location, and slightly improves the source location accuracy.

Downloaded from adb.sagepub.com at SEIR on August 2, 2012

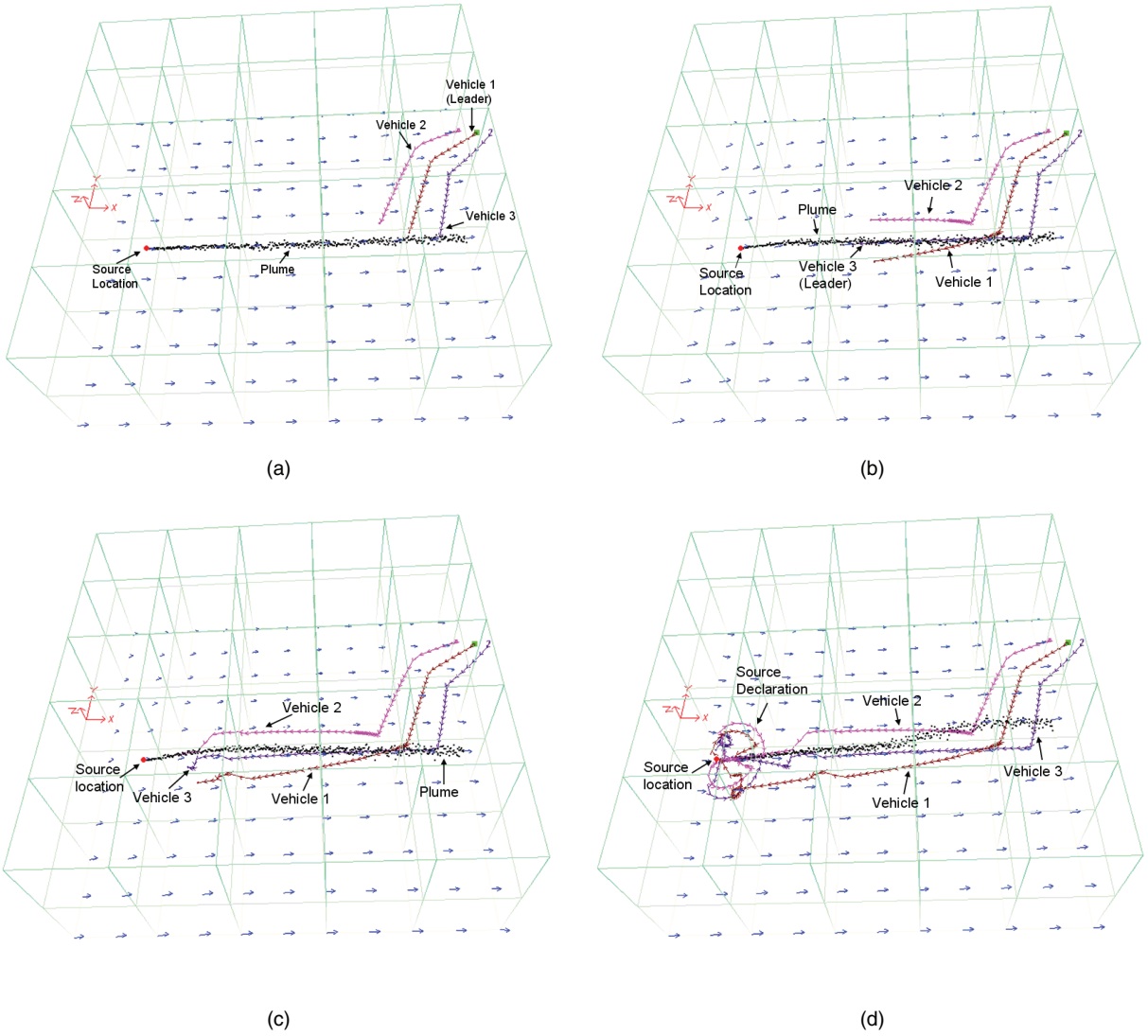

Figure 6. A test run of moth-inspired plume tracing via multiple vehicles under formation control. (a) Find-Plume activity: vehicle 1 is the leader, and vehicles 2 and 3 follow it to find the plume, but vehicle 3 becomes the leader when it first detects the plume. (b) Maintain-Plume activity: vehicle 3 is the leader to perform Maintain-Plume behavior, and vehicles 1 and 2 follow the leader toward to the source. (c) Reacquire-Plume activity: vehicle 2 first detects the plume during Reacquire-Plume and becomes the new leader, and vehicles 1 and 3 follow it toward to the source location. (d) Declare-Source activity: all vehicles run around the source location to identify the chemical source by alternating the leader and followers' roles.

Table 2. Time cost for chemical plume tracing (CPT) test runs on single vehicle versus multiple vehicles

CPT strategies (1000 runs)	Average time, s	Time within 150–200 s	Time within 200–250 s	Time within 250–300 s	Time within 300–350 s	Time within 350–400 s	Time greater than 400 s
Single vehicle	229.7512	61/1000 (6.1%)	754/1000 (75.4%)	164/1000 (16.4%)	16/1000 (1.6%)	5/1000 (0.5%)	0/1000 (0.0%)
Multiple vehicles	195.1064	645/1000 (64.5%)	329/1000 (32.9%)	21/1000 (2.1%)	2/1000 (0.2%)	2/1000 (0.2%)	1/1000 (0.1%)

6 Conclusions

This paper presents a novel strategy for a moth-inspired CPT via multiple AUVs under formation control. The leader in the vehicle fleet is responsible for finding the plume, tracing the plume, casting the plume, and declaring the source location, whereas the two followers serve as guarders keeping the leader in the middle when performing CPT missions. Figure 7 displays the trajectories from the home location to the

Downloaded from adb.sagepub.com at SEIR on August 2, 2012

Table 3. Source identification accuracy for chemical plume tracing (CPT) test runs on single vehicle versus multiple vehicles

CPT strategies (1000 runs)	Source declaration error, m	Estimated source location	Error within 0.0–0.5 m	Error within 0.5–1.0 m	Error within 1.0–1.5 m	Error within 1.5–2.0 m	Error greater than 2.0 m
Single AUV	0.2195	$\Delta\overline{X}$ =10.1460 m, $\Delta\overline{Y}$ =0.0018 m	878/1000 (87.8%)	87/1000 (8.7%)	28/1000 (2.8%)	6/1000 (0.6%)	1/1000 (0.1%)
Multiple AUVs	0.1782	$\Delta\overline{X}$ =10.1066 m, $\Delta\overline{Y}$ = – 0.0022 m	921/1000 (92.1%)	61/1000 (6.1%)	14/1000 (1.4%)	2/1000 (0.2%)	2/1000 (0.2%)

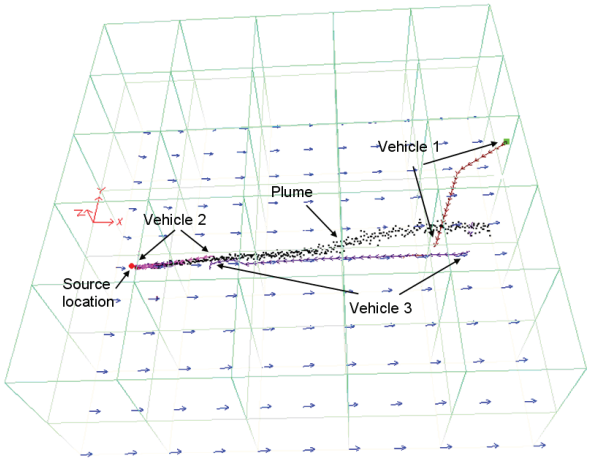

Figure 7. Trajectories generated by the leader vehicles during Find-Plume, Maintain-Plume, and Reacquire-Plume activities. Each segment of the trajectories shows a short distance to its target defined during the test run.

plume source location during the leaders' maneuvers. The leaders generate these nearly linear trajectories, which are close to the shortest paths to find the plume and to trace the plume toward its source location. The test run in Figure 6c shows that a follower (vehicle 2) detects the chemical plume and takes over the leader role when the leader (vehicle 1) activates the Reacquire-Plume behavior after it loses its contact with the plume for a certain number of seconds, so that the time cost for casting the plume on cloverleaf-shaped trajectories significantly decreases, i.e., the time cost for plume tracing is greatly reduced, as indicated in Table 2. The time cost for declaring the source location is also reduced because creating LCDPs in parallel by multiple vehicles allows the source declaration to be speeded up. The tracking of a chemical plume via multiple vehicles is more robust as oppose to a single vehicle, whereas if one vehicle is defective in the vehicle fleet the rest of vehicles can continue the CPT mission.

Compared with the cooperation mode of the previous multi-robot CPT strategies (e.g., Hayes et al., 2002; Meng et al., 2011), the main advantages of the leader–follower strategy are addressed below. First, the tracking of a plume with a significant meander using a non-leader–follower strategy may frequently activate the Reacquire-Plume behavior to cast the lost plume. However, the leader–follower strategy can eliminate a number of Reacquire-Plume activities, as one of the followers may still keep contact with the intermittent plume when the leader loses the plume. Furthermore, the vehicle fleet has an improved ability to maintain contact with the intermittent plume during the vehicles' role switch as they maneuver "in the intermittent plume" in different directions. The two simulation examples compare the plume-tracing trajectory created by the leader–follower strategy shown in Figure 8a and

Downloaded from adb.sagepub.com at SEIR on August 2, 2012

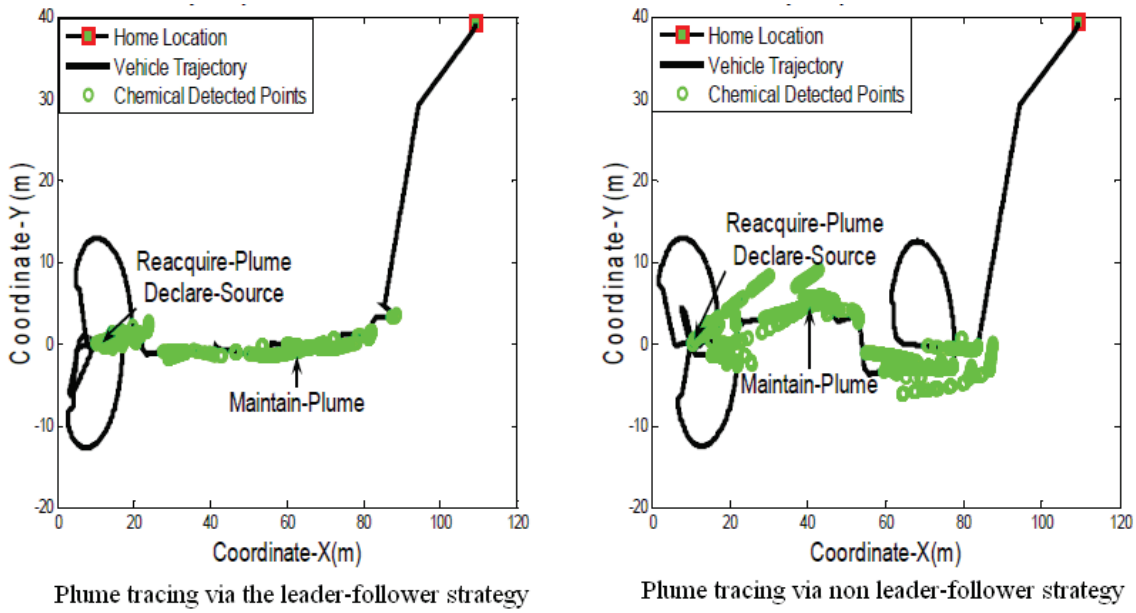

Figure 8. Comparison studies on plume tracing using the leader–follower and non-leader–follower strategies.

the one by the non-leader–follower strategy shown in Figure 8b. Clearly, the leader–follower strategy controls the vehicle fleet to travel a short distance to reach the source location. The coordination mechanisms of the non-leader–follower strategy evaluated in this study is comparable with those of the multi-robot CPT strategies (e.g., Hayes et al., 2002). Second, the leader–follower strategy also improves the source identification performance, whereas the multi-robot CPT strategies (e.g. Hayes et al., 2002; Marques et al., 2002) do not address this issue. Finally, the proposed strategy is evaluated by considering the vehicle dynamics, which significantly affects CPT performance.

For tracing a plume via multiple AUVs, there always exists a trade-off of determining AUVs number between the system cost and CPT performance. This study suggests that it would be enough to use three vehicles to trace a plume of the Rhodamine dyes developed in a turbulent, near-shore, oceanic fluid flow, which was used for in-water test runs, as shown in Figures 9a and 9b. Considering the AUV turning radius, we control distances of followers to the leader between 10 and 20 m to cover the Rhodamine dye plume with a width in the order of tens of meters. Adding any new vehicles into the multi-vehicles system requires that just the following distances of the new followers to the leader need to determine. Because the communication between AUVs is still a bottleneck for application of AUVs in ocean environments, we assume that communication between AUVs is available for developing the new algorithm. The algorithm suggests that the leader negotiates with the followers in a distributed way. Each individual vehicle behaves as a single independent moth-vehicle to trace the chemical plume when the communication link between the vehicles is broken.

This paper focuses on simulation evaluation on the proposed strategy. Differently from plume-tracing tests via mobile robots in environments with scales of a few meters, the proposed plume-tracing strategies, which are evaluated by using the simulated plume in an operational area with a large scale (over 100 m), address not only patchy odor concentrations but also significant plume meander. The significant plume meander is yielded when the plume is transported over a significant distance from its source location. The significant plume meander often causes a vehicle to lose contact with the plume because the instantaneous fluid flow direction within the plume with the significant meander is not always aligned with the plume's long axis because of the time lag of forming the plume. Our field tests were done by a direct transition from the simulated environment to the near-shore ocean environments.

The successful in-water test runs of tracing the Rhodamine dye plumes via a moth-inspired vehicle (Li et al., 2006; Farrell et al., 2005; Kang et al., 2011; Tian et al., 2011) support our design procedure, i.e., the moth-inspired CPT algorithms evaluated in the simulated environment are effective for tracing the Rhodamine dye plumes, as shown in Figures 9a and 9b, which were developed in the ocean environments at the San Clemente Island of California and at Dalian Bay in China, respectively. The width range of both plumes is about tens of meters.

Our further research will be to expand CPT missions via multiple vehicles from two dimensions to three dimensions. In particular for locating deep-sea

Downloaded from adb.sagepub.com at SEIR on August 2, 2012

(a) (b)

Figure 9. A single moth-inspired autonomous underwater vehicle (AUV) successfully tracked the Rhodamine dye plumes in November 2002 at the San Clemente Island of California in USA and October 2010 at Dalian Bay in China. (a)The Rhodamine dye plume was developed in the ocean environment at the San Clemente Island of California, USA. (b) The Rhodamine dye plume was developed in the ocean environment at Dalian Bay, China.

hydrothermal vents, we need to systemically evaluate the tracking of hydrothermal plumes with both buoyant and non-buoyant features.

Acknowledgements

The authors express their thanks to Professor Feng, Professor Li, and Dr Xu at the State Key Laboratory of Robotics at Shenyang Institute of Automation for their support in conducting this research. We also appreciate the suggestions of the reviewers, which have greatly improved the article.

Funding

The work of this paper is in part supported by the Chinese National 863 Plan Program under grant 2007AA09Z207, National Natural Science foundation under grants 61075085 and 41106085, and State Key Laboratory of Robotics at Shenyang Institute of Automation under grant 2009-Z03.

References

Basil, J., & Atema, J. (1994). Lobster orientation in turbulent odor plumes: Simultaneous measurements of tracking behavior and temporal odor patterns. *Biological Bulletin, 187*, 272–273.

Belanger, J. H., & Willis M. A. (1998). Adaptive control of chemical-guided location: Behavioral flexibility as an antidote to environmental unpredictability. *Adaptive Behavior, 4*, 217–253.

Cardé, R. T. (1996). Odour plumes and odour-mediated flight in insects. In *Olfaction in mosquito–host interactions* (pp. 54–70). CIBA Foundation Symposium 200. Chichester, UK: Wiley.

Cardé, R. T., & Willis M. A. (2008). Navigational strategies used by insects to find distant, wind-borne sources of odor. *Journal of Chemical Ecology, 34*, 854–866.

Cowen, E. A., & Ward, K. B. (2002). Chemical plume tracing. *Environmental Fluid Mechanics, 2*, 1–7.

Cui J. Z., Xu D. M., Xu Z., Yan W. S., & Pan Y. (2007). Simulation of autonomous underwater vehicles formation control Based on Simulink and VRML. *Journal of System Simulation, 19*(13), 2881–2884.

Edwards, D. B., Bean, T. A., Odell, D. L., & Anderson, M. J. (2004). A leader–follower algorithm for multiple AUV formations. *Proceedings of 2004 IEEE/OES Autonomous Underwater Vehicles*, Sebasco Estates, ME.

Elkinton, J. S., Schal C., Onto T., & Cardé R. T. (1987). Pheromone puff trajectory and upwind flight of male gypsy moths in a forest. *Physiological Entomology,12*, 399–406.

Farrell J. A., Murlis J., Long X., Li W., & Cardé R. T. (2002). Filament- based atmospheric dispersion model to achieve short time-scale structure of odor plumes. *Environmental Fluid Mechanics, 2*, 143–169.

Farrell J. A., Pang S., & Li W. (2005). Chemical plume tracing via an autonomous underwater vehicle. *IEEE Journal of Ocean Engineering, 30*, 428–442.

Grasso, F. W., Consi, T. R., Mountain, D. C., & Atema, J. (2000). Biomimetic robot lobster performs chemoorientation in turbulence using a pair of spatially separated sensors: Progress and challenges. *Robotics and Autonomous Systems, 30*, 115–131.

Hayes A. T., Martinoli A., & Goodman R. M. (2002). Distributed chemical source localization. *IEEE Sensors Journal, 2*, 260–271.

Ishida H., Kagawa Y., Nakamoto T., & Moriizumi T. (1996). Chemical source localization in the clean room by an autonomous mobile sensing system. *Sensors and Actuators B, 33*, 115–121.

Kang X. D. (2010). Research on chemical plume exploration via multiple AUVs with formation-keeping. Ph.D. dissertation, Shenyang Institute of Automation, Chinese Academy of Sciences.

Kang X. D., Li W., Xu H. L., Feng X. S., & Li Y. P. (2011). Validation of an odor source identification algorithm via an underwater vehicle. *2011 International Conference on Intelligent Systems Design and Engineering Applications* (in press).

Koehl M. A. R., Koseff J. R., Crimaldi J. P., McCay M. G., Cooper T., Megan B., Wiley M. B., & Moore P. A. (2001).

Downloaded from mms.sagepub.com at SERIALS on August 2, 2012

Lobster sniffing: Antennule design and hydrodynamic filtering of information in an odor plume. *Science, 294*, 1948–1951.

Li W. (2010). Identifying an odour source in fluid-advected environments, algorithm abstracted from moth-inspired plume tracing strategies. *Applied Bionics and Biomechanics*, *7*, 3–17.

Li W., Farrell J. A., & Cardé R. T. (2001). Tracking of fluid-advected chemical plumes: Strategies inspired by insect orientation to pheromone. *Adaptive Behavior, 9*, 143–170.

Li W., Farrell J. A., Pang S., & Arrieta R. M. (2006). Moth-inspired chemical plume tracing on an autonomous underwater vehicle. *IEEE Transactions on Robotics, 22*, 292–307.

Liao Q., & Cowen E. A. (2002). The information content of a scalar plume – A plume tracing perspective. *Environ Fluid Mechanics 2*, 9–34.

Lilienthal A. J., Ulmer H., Froehlich H., Werner F., & Zell A. (2004). Learning to detect proximity to a gas with mobile robot. *Proceedings of IEEE Conference on Intelligent Robots and Systems* (pp. 1444–1449).

Marques L., Nunes U., & Almeida A. T. de. (2002). Olfaction-based mobile robot navigation. *Thin Solid Films.,418*, 51–58.

Meng Q. H., Yang W. X., Wang Y., and Zeng M. (2011). Collective odor source estimation and search in time-variant airflow environments using mobile robots. *Sensors, 11*, 10415–10443.

Russell R. A. (2001). Tracking chemical plumes in constrained environments. *Robotica, 19*, 451–458.

Sutton J., & Li W. (2008). Development of CPT_M3D for multiple chemical plume tracing and source identification. *Seventh International Conference on Machine Learning and Applications* (pp. 470–475).

Tian Y., Li W., Zhang A. Q, & Yu J. C. (2011). Behavior-based control of an autonomous underwater vehicle for adaptive plume mapping. *The 2nd International Conference on Intelligent Control and Information Processing* (pp. 719–724).

Vergassola, M., Villermaux, E., & Shraiman B. I. (2007). "Infotaxis" as a strategy for searching without gradients. *Nature, 445*, 406–409.

Weissburg M. J., Dusenbery D. B., Ishida H., Janata J., Keller T., Roberts P. J. W., & Webster D. R. (2002). A multidisciplinary study of spatial and temporal scales containing information in turbulent chemical plume tracking. *Environmental Fluid Mechanics 2*, 65–94.

Weissburg, M. J., & Zimmer-Faust, R. K. (1994). Odor plumes and how blue crabs use them in finding prey. *Journal of Experimental Biology, 197*, 349–375.

Zarzhitsky D., & Spears D. F. (2005). Swarm approach to chemical source localization. *Proceedings of 2005 IEEE International Conference on Systems, Man and Cybernetics* (pp. 1435–1440).

About the Authors

Xiaodong Kang received his Ph.D. (2011) in pattern recognition and intelligent systems from the graduate school of the Chinese Academy of Sciences. Currently he is an engineer at Sany Heavy Industry Co., Ltd. and a postdoctoral researcher at Central South University, China. His current research interests include: intelligent systems, robotics, electro-hydraulic integration, and human–computer interaction. *E-mail:* kangxdcsu@163.com

Wei Li received his B.S. (1982) and M.S. (1984) in electrical engineering from the Northern Jiaotong University, Beijing, P.R. China, and a Ph.D. (1991) in electrical and computer engineering from the University of Saarland, Germany. He was a full professor of Computer Science and Technology, at Tsinghua University (1996–2001). Currently he is a Professor with the Department of Computer and Electrical Engineering and Computer Science at California State University, Bakersfield. Since 2009, Dr. Li has been appointed a Professor at the State Key Laboratory of Robotics, Shenyang Institute of Automation, Chinese Academy of Sciences.

Dr. Li received the 1995 National Award for Outstanding Postdoctoral Researcher in China and the 1996 Award for Outstanding Young Researcher at Tsinghua University. He was a Croucher Foundation Research Fellow (1996) at City University of Hong Kong and an Alexander von Humboldt Foundation Research Fellow at the Technical University of Braunschweig, Germany (1997–1999). From 1999 to 2001, he was a Research Scientist of the Department of Electrical Engineering at the University of California, Riverside. His research interests are bio-inspired intelligent systems, robotics, BCI-based control system, fuzzy logic control and neural networks, multisensor fusion and integration, and graphical simulation. *Address*: Department of Computer and Electrical Engineering and Computer Science at California State University, Bakersfield, Bakersfield, CA 93311, USA. *E-mail:* wli@cs.csubak.edu

Downloaded from adb.sagepub.com at SEIR on August 2, 2012